Supplemental Information

S-Nitrosylation—Mediated Redox Transcriptional Switch Modulates Neurogenesis and Neuronal Cell Death

Shu-ichi Okamoto, Tomohiro Nakamura, Piotr Cieplak, Shing Fai Chan, Evgenia Kalashnikova, Lujian Liao, Sofiyan Saleem, Xuemei Han, Rameez Zaidi, Arjay Clemente, Anthony Nutter, Sam Sances, Christopher Brechtel, Daniel Haus, Florian Haun, Sara Sanz-Blasco, Xiayu Huang, Hao Li, Jeffrey D. Zaremba, Jiankun Cui, Zezong Gu, Rana Nikzad, Anne Harrop, Scott McKercher, Adam Godzik, John R. Yates, III, and Stuart A. Lipton

Table of Contents
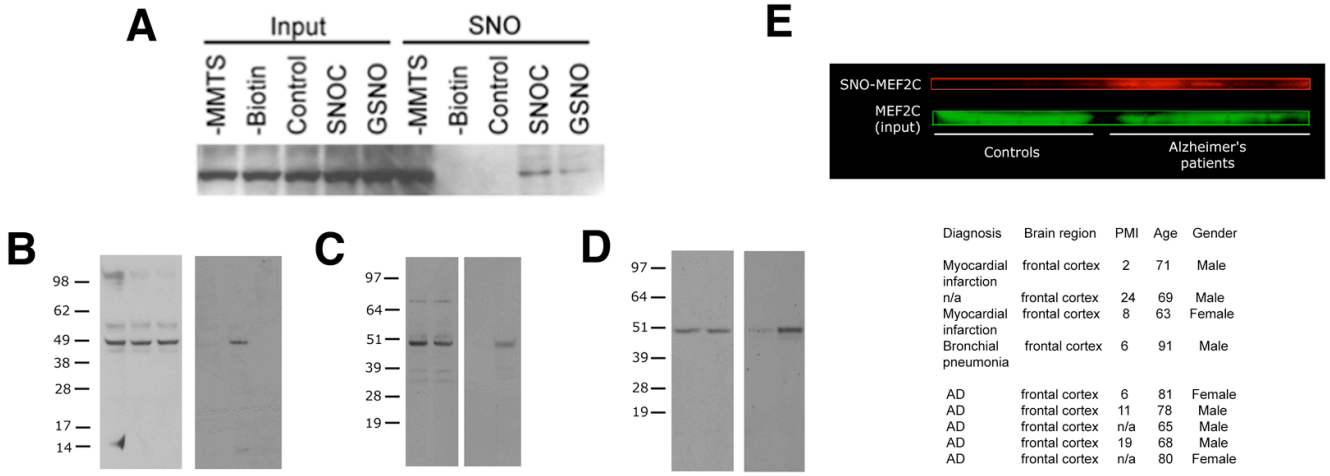
Figure S1 Detection of S-Nitrosylated MEF2C (related to Figure 1)
(A) Detection of S-nitrosylated (SNO-)MEF2C. HEK293T cells were transfected with myc-tagged MEF2C and incubated with the NO donors S-nitrosocysteine (SNOC) or nitroso-S-glutathione (GSNO). SNO-MEF2C levels were determined by biotin switch assay. SNO-MEF2C protein was immunoprecipitated and detected with anti-myc antibody.
(B–D) Full-length version of blots presented in Figure 1. (B) for Figure 1A, (C) for Figure 1B, and (D) for Figure 1C.
(E) Human postmortem brain tissue from control and Alzheimer's disease (AD) patients was subjected to the biotin switch assay to detect SNO-MEF2C. Bottom panel shows total MEF2C. Human samples used in this analysis are described in the Table below the blot. PMI, postmortem interval; AD, Alzheimer's disease; n/a, non-CNS cause of death.

A

B

C
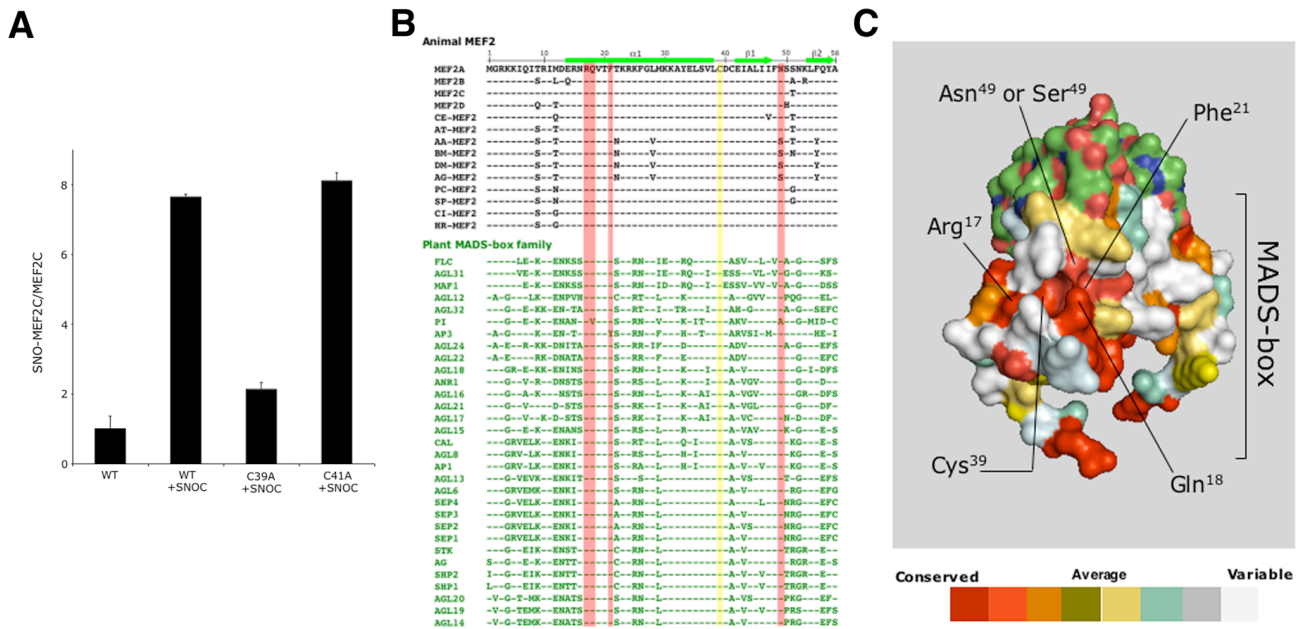
Figure S2 Quantification of SNO-MEF2C and Conservation of S-Nitrosylated Cys Residue Across Kingdoms (related to Figure 2)

(A) Relative quantification of S-nitrosylated wild-type MEF2C (WT), MEF2C(C39A) mutant, and MEF2C(C41A) mutant in HEK cells after exposure to SNOC. Bars represent mean + SEM of the ratio of SNO-MEF2 protein to total MEF2 protein expression. Biotin switch and immunoblot assays from which these histograms were calculated are presented in Figure 2B in the text.

(B and C) Conservation of Cys[39] and the surrounding residues among animal MEF2 proteins as well as other related MADS-family proteins extending into the plant kingdom. Sequence alignment (B) of the MADS-box DNA binding domains of MEF2. MEF2A-D; *Caenorhabditis elegans* CE-MEF2; *Achaearanea tepidariorum* AT-MEF2; *Aedes aegypti* AA-MEF2; *Bombyx mori* BM-MEF2; *Drosophila melanogaster* DM-MEF2; *Anopheles gambiae* AG-MEF2; *Podocoryne carnea* PC-MEF2; *Strongylocentrotus purpuratus* SP-MEF2; *Ciona intestinalis* CI-MEF2; *Halocynthia roretzi* HR–MEF2) and the type II MADS family in *Arabidopsis* (Ng and Yanofsky, 2001). α-Helix and β-strands are shown as bars and arrows, respectively. Cys[39] is colored yellow. Conserved residues inside the pocket are colored red. Surface representation (C) colored by conservation scores (red, most conserved; white, least conserved). The conservation scores were calculated using ConSurf (http://consurf.tau.ac.il) and visualized with PyMol. Scores are based on the CLUSTAL W alignment of the MADS box in both the animal and plant families displayed in (B).
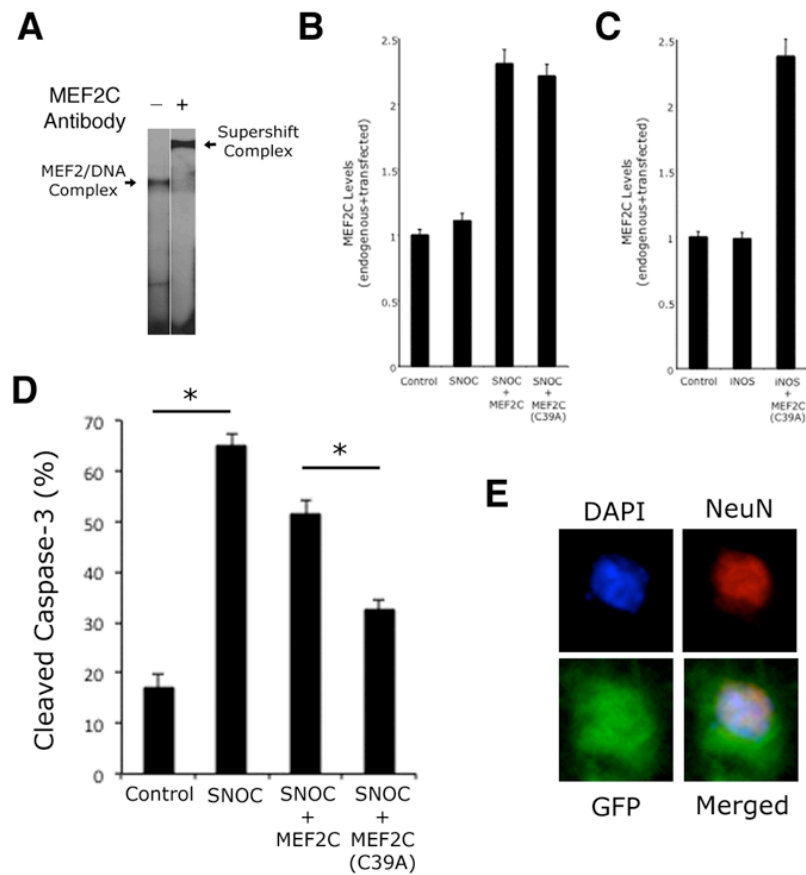
Figure S3 Analysis of MEF2 Binding to DNA, MEF2 Levels After Transfection, Apoptosis using Cleaved Caspase-3 Staining, and DAPI/NeuN/GFP Staining (related to Figure 3)

(A) Full-length blot and supershift of MEF2/DNA complex with MEF2C antibody on EMSA.

(B and C) Levels of endogenous plus transfected MEF2C, and MEF2C(C39A) under various conditions in cultured cortical neurons. The mean fluorescence intensity of specific immunosignals in transfected neurons was quantified by deconvolution fluorescence microscopy. The signal from empty vector-transfected (Control) cells was assigned a value of 1, and the other signals were expressed relative to this control. MEF2C levels (B) in SNOC-exposed neurons transfected with MEF2C or MEF2C(C39A). These constructs were used in the analysis of MEF2 transcriptional activity (Figure 3E) and neuronal apoptosis (Figure 3G). MEF2C levels (C) in iNOS-expressing neurons transfected with MEF2C(C39A). These constructs were used in the analysis of MEF2 transcription activity (Figure 3F).

(D) Neuronal cell death was assessed by staining for cleaved caspase-3 using a specific antibody. Bars represent mean + SEM (n = 9 cultures derived from three independent platings, *p < 0.0001 by ANOVA with post-hoc Scheffé's test).

(E) Representative image of NeuN/DAPI/GFP staining.

4
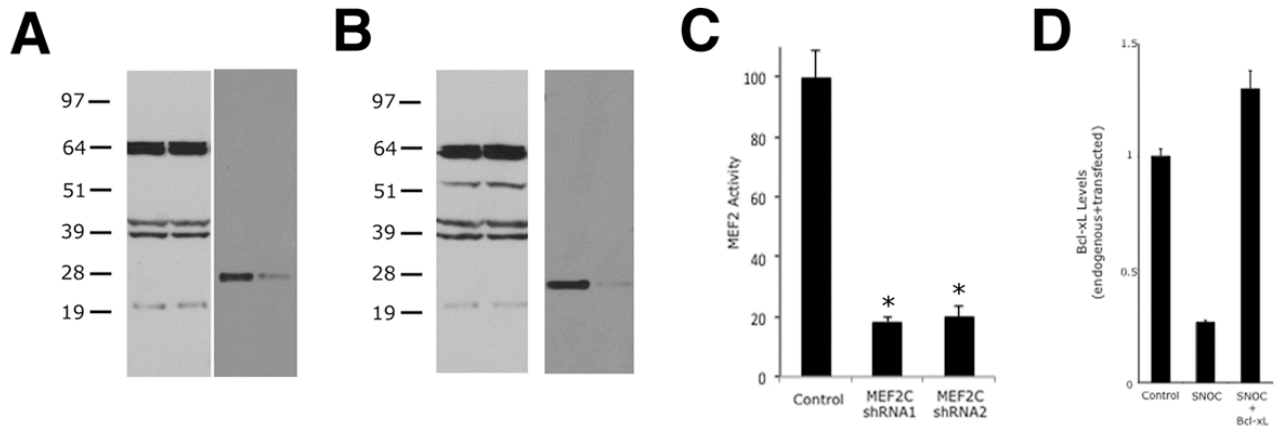
Figure S4 Analysis of Bcl-xL and MEF2 Expression (related to Figure 4)
(A and B) Full-length blots of Bcl-xL expression presented in Figures 4A and 4B, respectively.
(C) Knockdown of MEF2C with shRNA constructs attenuates MEF2-dependent transcriptional activity in cortical neurons. MEF2 luciferase reporter was cotransfected with control vector or MEF2C shRNA-expression vectors. Values are mean + SEM (n = 9 cultures derived from two independent platings, *p < 0.0001 by ANOVA with post-hoc Dunnett's test).
(D) Levels of endogenous plus transfected Bcl-xL under various conditions in cultured cortical neurons. The mean fluorescence intensity of specific immunosignals in transfected neurons was quantified by deconvolution fluorescence microscopy. The signal from empty vector-transfected (Control) cells was assigned a value of 1, and the other signals were expressed relative to this control. These constructs were used to determine the antiapoptotic effects of transfected Bcl-xL (Figure 4F).
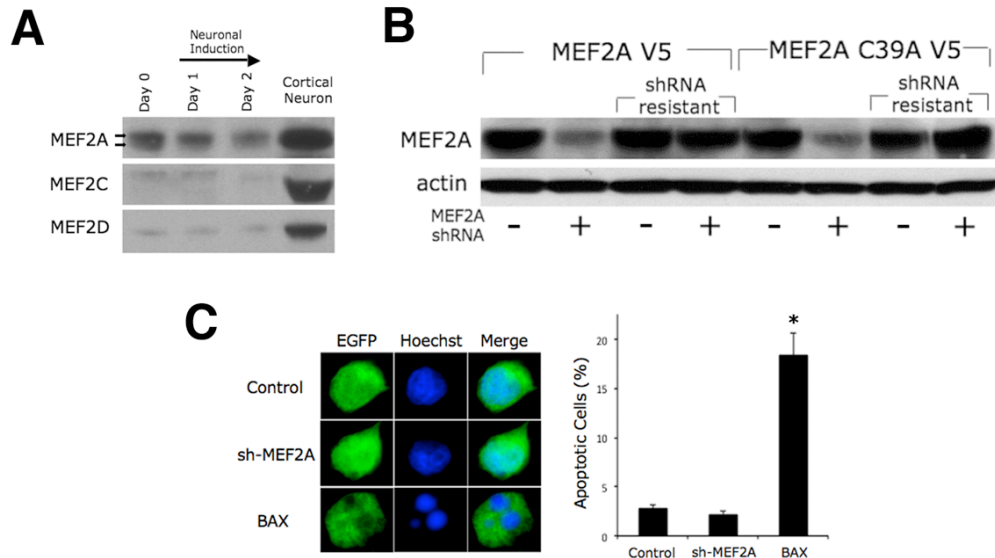
Figure S5 Analysis of MEF2 Expression and Effect on Apoptosis (related to Figure 5)

(A) Expression of MEF2 family members during neuronal differentiation of rat adult hippocampal progenitor/stem cells (NSCs). Immunoblot analysis of MEF2 protein expression in NSCs on the indicated day of neuronal induction. Lysates from rat cortical neurons served as a positive control.

(B) shRNA knockdown of MEF2A and rescue with shRNA-resistant MEF2A. HEK 293 cells were transfected with the indicated MEF2A constructs and shRNA expression vectors against MEF2A (+) or non-targeted sequences (–). MEF2A levels were determined by immunoblot using anti-V5 antibody. Actin levels shown to insure equal loading.

(C) MEF2A knockdown does not induce cell death in NSCs. NSCs were transfected with EGFP plus either control vector, shRNA against MEF2A (sh-MEF2A), or a BAX expression vector (representing a positive control to induce apoptosis). Representative images of EGFP-positive transfected cells. Apoptotic cell death was induced by BAX but not sh-MEF2A (mean + SEM, n = 8 cultures derived from two independent platings, *p < 0.0001 by ANOVA with post-hoc Dunnett's test).
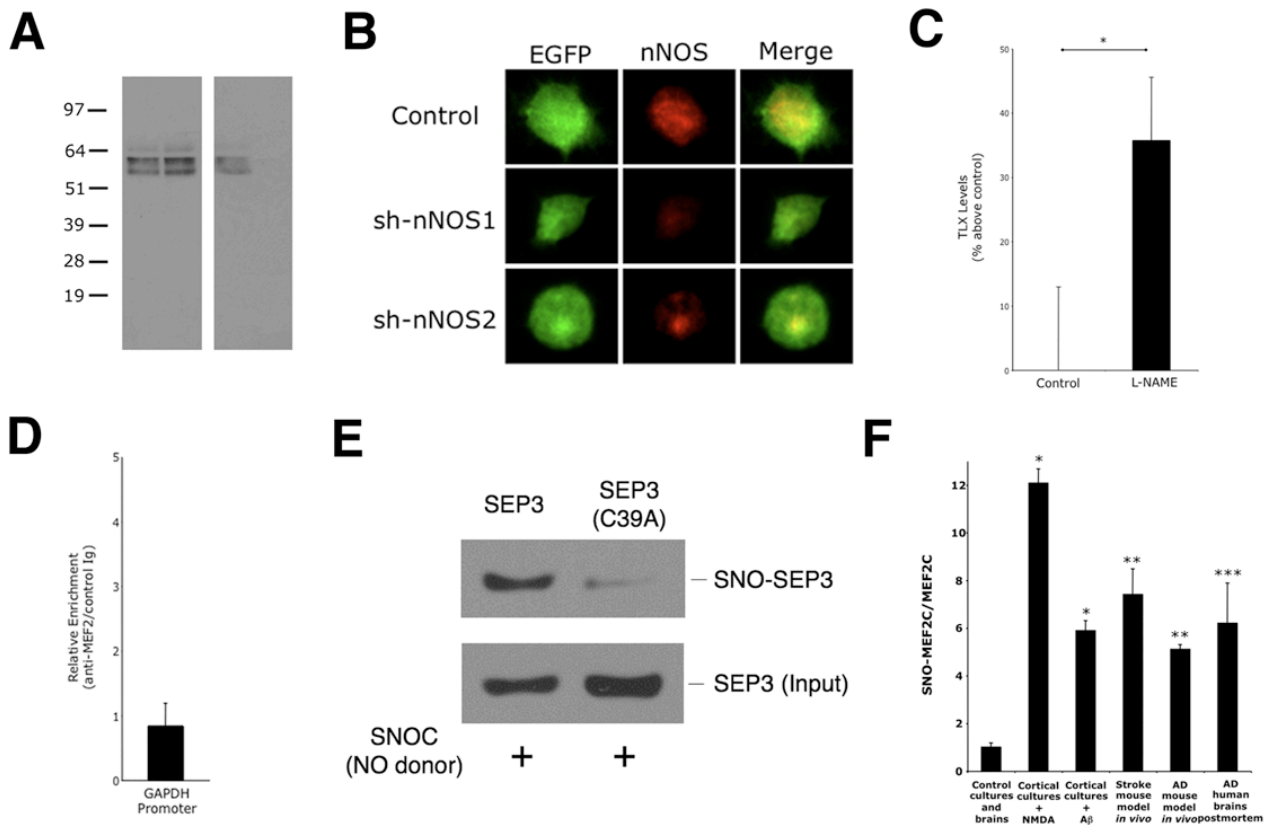
Figure S6 Analysis of SNO-MEF2 Family Members, NOS, and TLX Levels (related to Figure 6)

(A) Full-length blots of SNO-MEF2A by biotin switch assay presented in Figure 6B.

(B) Knockdown of nNOS using shRNA expression plasmids. Adult hippocampal progenitor/stem cells (NSCs) were transfected with control vector or a vector expressing one of two shRNAs for nNOS (sh-nNOS1 or sh-nNOS2). EGFP-positive transfected cells were stained with an antibody against nNOS.

(C) NOS inhibition increases TLX levels in mouse dentate gyrus. The NOS inhibitor, L-NAME, was systemically administered to adult mice for 5 d prior to collecting mRNA from the dentate gyrus for determination of TLX levels. mRNA was purified and analyzed using quantitative RT-PCR. Values represent mean percentage above basal TLX level + SEM (n = 3 animals for each group, $*p < 0.05$ by t test).

(D) As a control experiment for Fig. 6H, there was no enhancement on ChIP analysis of the GAPDH promoter using MEF2A antibody relative to control immunoglobulin (Ig) in rat adult NSCs. ChIP-PCR was performed on genomic DNA for the GAPDH promoter using normal rabbit Ig and MEF2A antibody. Values represent mean + SEM (n = 3 experiments).

(E) Cys^{39} of *Arabidopsis* MADS family protein SEP3 is S-nitrosylated. V5-tagged SEP3 and V5-tagged SEP3 with mutated Cys^{39} to Ala^{39} (SEP3(C39A)) were transfected into HEK293T cells. The HEK cells were subsequently incubated with the physiological NO

7

donor SNOC. S-Nitrosylation of wild-type SEP3 or SEP3(C39A) was determined by biotin switch assay. SNO proteins were precipitated and detected with anti-V5 antibody. (F) Relative amounts of SNO-MEF2C. Biotin switch assays and immunoblots were quantified, and the relative ratio of SNO-MEF2C to total MEF2C was calculated under each condition. Bars represents mean + SEM (n ≥ 3 for each group; *$p < 0.0001$, **$p < 0.001$, ***$p < 0.05$ by ANOVA with post-hoc Scheffé's test).

Supplemental Experimental Procedures

Plasmids and Lentiviral Vectors

Human MEF2C cDNA was cloned into pcDNA 3.1/*myc*-His(–) and pcDNA 3.1/V5-His to provide myc and V5 tags, respectively. Point mutations were introduced using the QuikChange Site-Directed Mutagenesis Kit (Stratagene). An inducible nitric oxide synthase (iNOS) expression vector was purchased from ATCC. Bcl-xL-promoter luciferase reporter was provided by Gabriel Nunez (University of Michigan) (Grillot et al., 1997). SEP3 cDNA was provided by Martin F. Yanofsky (UCSD). pStrike plasmid expressing shRNAs targeting MEF2A and non-silencing sequences were constructed according to the manufacturer's instructions (Promega). shRNA-resistant point mutations were introduced into the pCDNA-MEF2A vector with the QuikChange mutagenesis kit. Plasmids were transfected using Lipofectamine 2000 (Invitrogen). We used a previously described MEF2 luciferase reporter plasmid (Okamoto et al., 2002). The pRL-SV40 renilla reporter plasmid was purchased from Promega. Luciferase activity was determined using a dual-luciferase reporter assay system (Promega). We constructed MEF2C (LV-MEF2) and its C39A mutant (LV–C39A) in the lentiviral transfer vector pRRL-PGK promoter-IRES2-GFP-SIN18WPRE (LV–GFP), as previously described (Cho et al., 2011). High-titer lentiviral constructs (~10^{10} transducing units/ml) for in vivo injection were generated at the Viral Core of the Salk Institute for Biological Studies.

Cell Culture and Analysis

Human embryonic kidney (HEK) 293T, or HEK293 cells stably expressing neuronal nitric oxide synthase (nNOS) were grown in DMEM containing 10% FCS (Uehara et al.,

2006). Cerebrocortical neurons were harvested from E16 Sprague-Dawley rats and maintained as previously described (Okamoto et al., 2002). Neuronal apoptotic death was assessed with Hoechst staining for nuclear morphology. Adult rat hippocampal neural progenitor/stem cells (NSCs) were obtained from Fred H. Gage (Salk Institute for Biological Studies). Progenitors were maintained in DMEM/F12 medium with 1 mM L-glutamine, N2 supplement (Invitrogen), and bFGF (20 ng/ml). Neuronal differentiation was initiated with 1 μM retinoic acid, 5 μM forskolin, and 0.5% fetal bovine serum, as described previously (Gage et al., 1995; Palmer et al., 1997). Neuronal differentiation was initially assessed using anti-TuJ1 (Covance). For quantitative immunofluorescence analysis, fluorescent images were randomly selected and assessed using deconvolution microscopy (Zeiss Axiovert 100M with SlideBook 5.0 software) as previously described (Okamoto et al., 2007; Okamoto et al., 2009).

Focal Cerebral Ischemia

Mice were cared for following animal protocols approved by the Sanford-Burnham Medical Research Institute. The light/dark cycle in the vivarium was 12/12 h. Mice were housed in groups of 3 to 5 adults per cage. All animals were assigned and analyzed in a blinded manner. As described previously (Gu et al., 2002; Satoh et al., 2006), we used the intraluminal filament model of middle cerebral artery (MCA) occlusion for one hour to detect S-nitrosylation of MEF2C and for 90 min followed by 24 hour reperfusion to analyze cell death. Male mice (C57BL/6) were anesthetized with a mixture of isoflurane and 70% nitrous oxide/30% oxygen that was delivered through a nose cone; physiological parameters were monitored during the procedure. Occlusion of blood flow was monitored by laser Doppler flowmetry. Lentiviral vectors (LV–GFP, LV–MEF2, or

LV–C39A) were stereotactically injected into the ipsilateral striatum (coordinates from bregma in mm: AP - 1.0, ML -2.5, DV -3.5) 3 weeks prior to MCA occlusion. After a 14-h reperfusion, mice were sacrificed for histological analysis. Sections were stained for DAPI, NeuN (EMD Millipore, MAB377), and GFP (Invitrogen, A-11122). In the penumbra, we stereologically scored and counted condensed, apoptotic nuclei in uninfected (GFP-negative/NeuN-positive) neurons vs. infected (GFP-positive/NeuN-positive) neurons for each construct and plotted the ratio in each case as an index of cell survival engendered by that genetic construct.

Human Brain Tissue

Human brain samples were provided by neuropathologist Eliezer Masliah (UCSD) and analysed with Institutional permission under State of California and NIH guidelines. Informed consent was obtained according to procedures approved by the UCSD and Sanford-Burnham Institutional Review Boards.

In Vivo BrdU or EdU Labeling and Histological Quantification of Neurogenesis

To assess the effect of MEF2A on adult neurogenesis, eight 4 to 6-month old male MEF2A KO mice and wild-type mice were injected intraperitoneally for 10 d with a daily dose of 50 mg/kg BrdU or EdU, and then sacrificed four weeks after the last injection. All animals were assigned and analyzed in a blinded manner. For the non-nitrosylatable MEF2 rescue studies of neurogenesis in AD model mice, we administered EdU for 5 days to ~6 month-old Tg2576 AD mice, followed by stereotactic injection of control lentivirus (LV–GFP) into the dentate gyrus (the specific area for adult neurogenesis that was to be evaluated) in the right hemisphere of each animal. Simultaneously, we

injected the left dentate gyrus with either LV–MEF2 and LV–C39A (coordinates from bregma in mm: AP -2.5, ML + and - 2.0, DV -2.0). The mice were then sacrificed four weeks following lentiviral injection. Brains were processed as described (Okamoto et al., 2007). In brief, tissues were cut into 40 µm-thick sections using a sliding microtome. We performed immunostaining on free-floating sections using Click-iT (for EdU staining) or anti-BrdU (Accurate Chemical, BU1/75 (ICR1)), plus anti-S100ß (Sigma, S2644), anti-NeuN (EMD Millipore, MAB377), and anti-GFP (Invitrogen, A-11122) antibodies. Visualization of immunofluorescence was performed using deconvolution microscopy (Zeiss Axiovert 100M with SlideBook 5.0 software).

Top-Down Analysis of MEF2C Protein by LTQ-Orbitrap-XL Mass Spectrometry

Recombinant MEF2C DNA-binding domain peptide (residues 1–93) was desalted on a MacroTrap Column (Michrom Bioresources), and eluted with buffer containing 5% acetic acid and 70% methanol to facilitate electrospray ionization. MEF2C protein (100 µg) was incubated with 20 µM of the physiological NO donor S-nitrosocysteine (SNOC) at RT in the dark. The mixture was then infused into an LTQ (linear trap quadrupole)-Orbitrap-XL mass spectrometer with ETD (electron transfer dissociation; Thermo Electron) by a syringe at a flow rate of 3 µl/min. The Orbitrap analyzer was used to obtain molecular ion spectra of either untreated or SNOC-exposed MEF2C. The resolution was set at 60,000 at 400 m/z for MS scans, and the AGC target value was set at 500,000. Multiply charged precursors (+16~+17) were accumulated with >100 microscans to obtain high signal-to-noise spectra and to compare the molecular ions before and after SNOC exposure.

Biotin Switch Assay

The biotin switch assay was performed in virtual darkness as previously described (Jaffrey and Snyder, 2001; Nakamura et al., 2010; Uehara et al., 2006; Yao et al., 2004). In brief, HEK 293T cell lysates were prepared in HENTS buffer (250 mM HEPES, pH 7.4, 1 mM EDTA, 0.1 mM neocuproine, 1% Triton X–100, and 0.1% SDS). Cell lysates were diluted to 1 mg/ml with HEN buffer (250 mM Hepes, pH 7.4, 1 mM EDTA, and 0.1 mM neocuproine); typically 500 µg of cell lysate was used for each assay. Four volumes of blocking buffer [2.5% SDS and 5 mM methyl methane thiosulfonate (MMTS) in HEN buffer] were mixed with the samples and incubated for 20 min at 50 °C to block free thiol groups. After removing excess MMTS by acetone precipitation, S-nitrosothiols were chemically reduced to free thiol groups with 1 mM ascorbate. Newly-formed thiols were then labeled with the sulfhydryl-specific biotinylating reagent *N*-[6-biotinamido]-hexyl]-1'-(2'pyridyldithio) propionamide (Pierce) at RT for 60 min. Proteins were precipitated with 50% acetone, and the pellets washed with acetone. Precipitates were resuspended in 100 µl of HENS buffer (HEN containing 1% SDS) and 200 µl of neutralization buffer (25 mM HEPES, 100 mM NaCl, 1 mM EDTA, and 0.5% Triton X-100). Fifteen to twenty microliters of this suspension were reserved for immunoblots to confirm equal loading. Biotinylated proteins were pulled down with Streptavidin-agarose beads (Pierce) at 4 °C overnight, and then washed 3 to 5 times with neutralization buffer. Proteins were eluted with LDS sample buffer (Invitrogen) containing 100 mM dithiothreitol (DTT) for 5 min at 95 °C. The eluent was separated on a 4-12% NuPAGE gel (Invitrogen) and immunoblotted for MEF2A (Santa Cruz, sc-313) or MEF2C (Aviva, ARP37342).

Fluorometric Detection of S-Nitrosylation

S-Nitrosothiol formation was detected by conversion of 2,3-diaminonaphthalene (DAN) to the fluorescent compound 2,3-naphthyltriazole (NAT) with an emission wavelength of 450 nm and an excitation wavelength of 375 nm using a fluorometric plate reader (Molecular Devices) as previously described (Gu et al., 2002; Uehara et al., 2006; Wink et al., 1999; Yao et al., 2004). The DAN assay was used on MEF2C protein purified from cells. For this purpose, HEK cells stably expressing neuronal NO synthase were transfected with wild-type V5-MEF2C or mutant V5-MEF2C(C39A). Two days later, cells were incubated with or without 5 µM A23187 for 6 h, and lysed in 400 µl of lysis buffer (PBS, pH7.4 containing 1% glycerol and 1% Triton X-100). SNO-MEF2C was immunoprecipitated with anti-V5 antibody (EMD Millipore, AB3792) in the dark, and the immunocomplex washed three times with lysis buffer. After resuspension of the immunocomplex in 100 µl of PBS, $HgCl_2$ and DAN were added to a final concentration of 200 µM each and incubated at RT for 30 min. The fluorescence intensity of the supernatant was measured using a fluorometric plate reader.

Electrophoreticmobility Shift Assay (EMSA)

Nuclear extracts and in vitro-translated MEF2C(C39A) protein were prepared as previously described (Okamoto et al., 2000; Okamoto et al., 2002). EMSAs were performed as previously reported (Krainc et al., 1998; Leifer et al., 1993).

Chromatin Immunoprecipitation (ChIP) Assay

ChIP analysis was performed as described previously with minor modifications (Flavell et al., 2006; Impey et al., 2004; Shalizi et al., 2006). In brief, $5–10 \times 10^6$ cells were fixed

with 1% formaldehyde. After rinsing with PBS, cells were harvested in 10 mM Tris-HCl

(pH 9.4) and 1 mM DTT, and then lysed in lysis buffer (0.1% SDS, 0.5% Triton X-100,

20 mM Tris–HCl at pH 8.1, and 150 mM NaCl). Samples were sonicated with six 30-s

pulses at half-minute intervals. Normal rabbit IgG (2 μg) or anti-MEF2 antibody (Santa

Cruz, sc-313) was used for overnight immunoprecipitation at 4°C. Immune complexes

were precipitated using Dynabeads Protein A (Invitrogen). Beads were washed

sequentially using lysis buffer, LiCl buffer, and TE (Tris-EDTA) buffer. Precipitants were

eluted in 1% SDS and 0.1 M NaHCO$_3$ (pH 8). Crosslinking was reversed overnight at

65°C. DNA was purified using a QIAquick PCR DNA purification spin column (Qiagen)

and subjected to PCR.

Geometry Optimization of the S-Nitrosylated MEF2-DNA Complex

For quantum mechanical calculations of the NO-modified cysteine residue, a molecular

model was constructed using the structure of the MEF2A-DNA complex, PDB ID:

1EGW. The Cys[39] residues in both polypeptide chains of the homodimer were modified

to CysNO. The following procedure was applied to derive atomic charges for the

modified CysNO. First, the geometry of the isolated CysNO dipeptide molecule (e.g.,

CH$_3$CO-NH-CHCH$_2$SNO-CO-NHCH$_3$) in the extended conformation was optimized

using the quantum mechanical GAMESS program (Schmidt et al., 1993). The program

generates the electrostatic potential (ESP) around the molecule. Then the atomic

charges were derived by fitting them to the quantum mechanically derived ESP using

the RESP method (Bayly et al., 1993) and R.E.D.III program (Grivel et al.). Geometry

optimization of the MEF2-DNA complex with modified Cys[39] was performed using

AMBER, a classical molecular mechanical program (Case et al., 2005), and its force field (Cornell et al., 1995). Figures were constructed using DS-Visualizer (Accelrys).

hESC Culture, Neural Induction and Transfection

We cultured and induced neural differentiation of H9 hESCs (WiCell Research Institute) as previously described (Cho et al., 2011). We transfected the cells with MEF2CA- or MEF2DN-tdTomato mammalian-expression constructs by electroporation using the human stem cell nucleofector® kit, according to the manufacturer's instructions (Lonza/Amaxa Biosystem).

mRNA Profiling by Microarray Analysis

We extracted total RNA from NSCs using Trizol Reagent and the PureLink™ RNA Mini Kit (Invitrogen). We prepared and labeled cRNA from 500 ng of RNA using the Illumina® RNA amplification kit from Ambion (Life technology). We then hybridized the labeled cRNA (750 ng) overnight, at 58 °C, to Sentrix® humanHT-12 Expression BeadChips (> 46,000 gene transcripts; Illumina), following the manufacturer's instructions. We subsequently washed and developed BeadChips with fluorolink streptavidin- Cy3 (GE Healthcare), and used an Illumina BeadArray Reader to scan the BeadChips. Microarray data were collected and analyzed in three steps. First, we obtained the sample probe file of all samples using illumina's GenomeStudio software after expression intensities were calculated and quality controlled with a detection p value set to < 0.05 for each gene probed on the array for all hybridizations. Second, we used hierarchical clustering methods to detect outliers in all samples. From this analysis no outliers were detected. Finally, we further analyzed the expression data for

differentially expressed genes using Agilent's GeneSpring GX 11.5 software with

quantile normalization, log transformation, and statistical analysis. We determined

differentially expressed genes on the basis of t tests with the Benjamini-Hochberg

correction (corrected P value ≤ 0.05) and fold-change difference in expression level

(fold change ≥ 1.5), as is customary for this analysis (Bolstad et al., 2003).

SUPPLEMENTAL REFERENCES

Accelrys, D.S. Visualizer, v16, Accelrys, Inc wwwaccelryscom.

Bayly, C.I., Cieplak, P., Cornell, W., and Kollman, P.A. (1993). A well-behaved electrostatic potential based method using charge restraints for deriving atomic charges: the RESP model. J. Phys. Chem. *97*, 10269 - 10280.

Bolstad, B.M., Irizarry, R.A., Astrand, M., and Speed, T.P. (2003). A comparison of normalization methods for high density oligonucleotide array data based on variance and bias. Bioinformatics *19*, 185-193.

Case, D.A., Cheatham, T.E., 3rd, Darden, T., Gohlke, H., Luo, R., Merz, K.M., Jr., Onufriev, A., Simmerling, C., Wang, B., and Woods, R.J. (2005). The Amber biomolecular simulation programs. J. Comput. Chem. *26*, 1668-1688.

Cho, E.G., Zaremba, J.D., McKercher, S.R., Talantova, M., Tu, S., Masliah, E., Chan, S.F., Nakanishi, N., Terskikh, A., and Lipton, S.A. (2011). MEF2C enhances dopaminergic neuron differentiation of human embryonic stem cells in a parkinsonian rat model. PLoS One *6*, e24027.

Cornell, W.D., Cieplak, P., Bayly, C.I., Gould, I., K.M. Merz, J., Ferguson, D., Spellmeyer, D.C., Fox, T., Caldwell, J.W., and Kollman, P.A. (1995). J. Am. Chem. Soc. *117*, 5179-5197.

Flavell, S.W., Cowan, C.W., Kim, T.K., Greer, P.L., Lin, Y., Paradis, S., Griffith, E.C., Hu, L.S., Chen, C., and Greenberg, M.E. (2006). Activity-dependent regulation of MEF2 transcription factors suppresses excitatory synapse number. Science *311*, 1008-1012.

Gage, F.H., Coates, P.W., Palmer, T.D., Kuhn, H.G., Fisher, L.J., Suhonen, J.O., Peterson, D.A., Suhr, S.T., and Ray, J. (1995). Survival and differentiation of adult

neuronal progenitor cells transplanted to the adult brain. Proc. Natl. Acad. Sci. USA *92*, 11879-11883.

Grillot, D.A., Gonzalez-Garcia, M., Ekhterae, D., Duan, L., Inohara, N., Ohta, S., Seldin, M.F., and Nunez, G. (1997). Genomic organization, promoter region analysis, and chromosome localization of the mouse bcl-x gene. J. Immunol. *158*, 4750-4757.

Grivel, N., Cieplak, P., and Dupradeau, F.-Y. REDIII, (RESP ESP charge Derive program), http://wwwq4md-forcefieldtoolsorg/RED/.

Gu, Z., Kaul, M., Yan, B., Kridel, S.J., Cui, J., Strongin, A., Smith, J.W., Liddington, R.C., and Lipton, S.A. (2002). S-Nitrosylation of matrix metalloproteinases: signaling pathway to neuronal cell death. Science *297*, 1186-1190.

Impey, S., McCorkle, S.R., Cha-Molstad, H., Dwyer, J.M., Yochum, G.S., Boss, J.M., McWeeney, S., Dunn, J.J., Mandel, G., and Goodman, R.H. (2004). Defining the CREB regulon: a genome-wide analysis of transcription factor regulatory regions. Cell *119*, 1041-1054.

Jaffrey, S.R., and Snyder, S.H. (2001). The biotin switch method for the detection of S-nitrosylated proteins. Sci. STKE *2001*, pl1-pl9.

Krainc, D., Bai, G., Okamoto, S., Carles, M., Kusiak, J.W., Brent, R.N., and Lipton, S.A. (1998). Synergistic activation of the N-methyl-D-aspartate receptor subunit 1 promoter by myocyte enhancer factor 2C and Sp1. J. Biol. Chem. *273*, 26218-26224.

Leifer, D., Krainc, D., Yu, Y.T., McDermott, J., Breitbart, R.E., Heng, J., Neve, R.L., Kosofsky, B., Nadal-Ginard, B., and Lipton, S.A. (1993). MEF2C, a MADS/MEF2-family transcription factor expressed in a laminar distribution in cerebral cortex. Proc. Natl. Acad. Sci. USA *90*, 1546-1550.

Nakamura, T., Wang, L., Wong, C.C., Scott, F.L., Eckelman, B.P., Han, X., Tzitzilonis, C., Meng, F., Gu, Z., Holland, E.A.*, et al.* (2010). Transnitrosylation of XIAP regulates caspase-dependent neuronal cell death. Mol. Cell *39*, 184-195.

Ng, M., and Yanofsky, M.F. (2001). Function and evolution of the plant MADS-box gene family. Nat. Rev. Genet. *2*, 186-195.

Okamoto, S.-i., Kang, Y.-J., Brechtel, C.W., Siviglia, E., Russo, R., Clemente, A., Harrop, A., McKercher, S., Kaul, M., and Lipton, S.A. (2007). HIV/gp120 decreases adult neural progenitor cell proliferation via checkpoint kinase-mediated cell-cycle withdrawal and G1 arrest. Cell Stem Cell *1*, 230-236.

Okamoto, S.-i., Krainc, D., Sherman, K., and Lipton, S.A. (2000). Antiapoptotic role of the p38 mitogen-activated protein kinase-myocyte enhancer factor 2 transcription factor pathway during neuronal differentiation. Proc. Natl. Acad. Sci. USA *97*, 7561-7566.

Okamoto, S.-i., Li, Z., Ju, C., Schölzke, M.N., Mathews, E., Cui, J., Salvesen, G.S., Bossy-Wetzel, E., and Lipton, S.A. (2002). Dominant-interfering forms of MEF2 generated by caspase cleavage contribute to NMDA-induced neuronal apoptosis. Proc. Natl. Acad. Sci. USA *99*, 3974-3979.

Okamoto, S.-i., Pouladi, M.A., Talantova, M., Yao, D., Xia, P., Ehrnhoefer, D.E., Zaidi, R., Clemente, A., Kaul, M., Graham, R.K.*, et al.* (2009). Balance between synaptic versus extrasynaptic NMDA receptor activity influences inclusions and neurotoxicity of mutant huntingtin. Nat. Med. *15*, 1407-1413.

Palmer, T.D., Takahashi, J., and Gage, F.H. (1997). The adult rat hippocampus contains primordial neural stem cells. Mol. Cell. Neurosci. *8*, 389-404.

Satoh, T., Okamoto, S.I., Cui, J., Watanabe, Y., Furuta, K., Suzuki, M., Tohyama, K., and Lipton, S.A. (2006). Activation of the Keap1/Nrf2 pathway for neuroprotection by electrophilic [correction of electrophillic] phase II inducers. Proc. Natl. Acad. Sci. USA *103*, 768-773.

Schmidt, M.W., Baldridge, K.K., Boatz, J.A., Elbert, S.T., Gordon, M.S., Jensen, J.H., Koseki, S., Matsunaga, N., Nguyen, K.A., Su, S.*, et al.* (1993). General atomic and molecular electronic structure system. J. Comput. Chem. *14*, 1347-1363.

Shalizi, A., Gaudilliere, B., Yuan, Z., Stegmuller, J., Shirogane, T., Ge, Q., Tan, Y., Schulman, B., Harper, J.W., and Bonni, A. (2006). A calcium-regulated MEF2 sumoylation switch controls postsynaptic differentiation. Science *311*, 1012-1017.

Uehara, T., Nakamura, T., Yao, D., Shi, Z.Q., Gu, Z., Ma, Y., Masliah, E., Nomura, Y., and Lipton, S.A. (2006). S-Nitrosylated protein-disulphide isomerase links protein misfolding to neurodegeneration. Nature *441*, 513-517.

Wink, D.A., Vodovotz, Y., Grisham, M.B., DeGraff, W., Cook, J.C., Pacelli, R., Krishna, M., and Mitchell, J.B. (1999). Antioxidant effects of nitric oxide. Methods Enzymol. *301*, 413-424.

Yao, D., Gu, Z., Nakamura, T., Shi, Z.Q., Ma, Y., Gaston, B., Palmer, L.A., Rockenstein, E.M., Zhang, Z., Masliah, E.*, et al.* (2004). Nitrosative stress linked to sporadic Parkinson's disease: S-Nitrosylation of parkin regulates its E3 ubiquitin ligase activity. Proc. Natl. Acad. Sci. USA *101*, 10810-10814.